Journal of Biochemistry and Molecular Biology, Vol. 40, No. 6, November 2007, pp. 1050-1057

JOURNAL OF Biochemistry and Molecular Biology

Characterization of Peptide Deformylase2 from *B. cereus*

Joon Kyu Park[1,2], Kook-Han Kim[1], Jin Ho Moon[1] and Eunice EunKyeong Kim[1,*]

[1]Life Sciences Division, Korea Institute of Science and Technology, 39-1 Hawolkok-dong, Sungbuk-gu, Seoul 136-791, Korea

[2]College of Life Sciences and Biotechnology, Korea University, Anam-dong, Sungbuk-gu, Seoul 136-701, Korea

Received 6 August 2007, Accepted 29 August 2007

Peptide deformylase (PDF) is a metalloenzyme that removes the N-terminal formyl groups from newly synthesized proteins. It is essential for bacterial survival, and is therefore-considered as a potential target for antimicrobial chemotherapy. However, some bacteria including medically relevant pathogens possess two or more def-like genes. Here we have examined two PDFs from *Bacillus cereus*. The two share only 32% sequence identity and the crystal structures show overall similarity with PDF2 having a longer C-terminus. However, there are differences at the two active sites, and these differences appear to contribute to the activity difference seen between the two. *Bc*PDF2 is found as a dimer in the crystal form with two additional actinonin bound at that interface.

Keywords: Actinonin complex, *Bacillus cereus*, Crystal structure, Peptide deformylase

Introduction

The emergence of drug resistance has brought the search for a new class of antibacterial agents with novel modes of action. One of the new targets recently receiving attention from both academic and industrial research groups is peptide deformylase (PDF, EC 3.5.1.88) (Zhang *et al.*, 2005; Leeds and Dean, 2006; Yuan and White, 2006). It is a metalloprotease that removes the N-terminal formyl groups from newly synthesized proteins and this step is required before the removal of N-terminal methionine in protein. The PDF activity is reported to be essential for bacterial survival (Ball and Kaesberg, 1973) yet the function of its homologues in animals and humans (Giglione *et al.*, 2000) is not clear, thereby PDF has been considered as a potential target in antimicrobial chemotherapy. Although the inhibitors of peptide deformylase have yet to be proven as antibacterial drugs, there have been a number of inhibitors reported targeting PDF (Jain *et al.*, 2005) and BB-83698 (Lofland *et al.*, 2004) and LBM415 (Ednie *et al.*, 2004) were entered into Phase I clinical trial in humans. Actinonin containing hydroxamic moiety is a naturally occurring pseudo-peptide. It is known to be highly potent (K_i = 0.28 nM for *Escherichia coli* PDF), and has been served as the basis for many inhibitors (Chen *et al.*, 2000).

Both biochemical and structural studies on various PDFs have shown that they share close enzymatic properties and overall structures in spite of rather low sequence homology (Guilloteau *et al.*, 2002). They have been grouped into two subfamilies, type I being represented by the *E. coli* enzyme (Becker *et al.*, 1998) and the type II by *Staphylococcus aureus* enzyme based on amino acid sequence similarities (Baldwin *et al.*, 2002). Most of bacteria possess only one gene coding PDF, but some eubacteria, especially Gram-positive bacteria, possesses more than one gene. For example, *Bacillus subtilis*, *Bacillus anthracis*, *Bacillus stearothermophillus*, and *Enterococcus faecalis* are reported to have two while *Streptomyces coelicolor* has four (Guilloteau *et al.*, 2002). In case of *S. aureus* and S. *pneumoniae* only one of the two genes is reported to be responsible for peptide deformylation (Margolis *et al.*, 2000; Margolis et al, 2001), while both products from *B. subtilis* are reported to exhibit similar enzymatic properties suggesting that both enzymes need to be inhibited in order to be effective therapeutic (Haas *et al.*, 2001).

Similar to *B. subtilis* there are two *def* genes reported for *Bacillus cereus* which is one of the major pathogens causing food poisoning (Srivaths *et al.*, 2004). The encoded proteins, PDF1 and PDF2 from *B. cereus*, share only 32% sequence identity and PDF1 is comprised of only 156 amino acids, while PDF2 has 184 amino acids (Fig. 1). Here we report the crystal structure of PDF2 from *B. cereus* in actinonin bound form and compared it with the recently reported structure of PDF1 from *B. cereus* (Moon *et al.*, 2005). Actinonin is known to be active against both Gram-positive and Gram-negative bacteria.

*To whom correspondence should be addressed.
Tel: 82-2-958-5937; Fax 82-2-958-5909
E-mail: eunice@kist.re.kr

Materials and Methods

Protein expression and purification. The *B.cereus def2* gene (Swiss Protein: Q819K2) encodes a 184 residues long protein. PDF2 from *B.cereus* ATCC 14579 was amplified by the polymerase chain reaction (PCR) using the genomic DNA as a template. The primers used were 5'-GCC GTG ACG CAT ATG CTT ACA ATG AAA GAT GTT ATT CGC-3' and 5'-GCT AGG CAT CTC GAG TCA TCG CTC TAG AGG TTT GGA ATC-3'. The PCR product was digested with *Nde*I and *Xho*I (NEB) and was then inserted into the *Nde*I/*Xho*I-digested expression vector pET-28a (Novagen), which added a hexa-histidine tag at the N-terminus of the recombinant *Bc*PDF2. The protein was over-expressed in *E. coli* BL21(DE3) cells containing kanamycin antibiotics. The cells were grown in Luria-Bertani medium to an OD_{600} of 0.5 at 310K and expression of the recombinant enzyme was induced by 0.5 mM isopropyl β-D-thiogalactopyranoside at 291K. Also added was 100 mM $ZnSO_4$. Cell growth continued at 291K for 16 h after the induction and cells were harvested by centrifugation at 5000 rev min^{-1} (Sorvall GSA rotor, Analytical Instruments, Golden Valley, MN, USA) for 30 min at 277K.

The cell pellet was resuspended in ice-cold lysis buffer (50 mM Tris-HCl pH 7.4, 300 mM NaCl, and 2 mM β-mercaptoethanol) and added 0.1 mM PMSF then homogenized by sonication. The crude lysate was centrifuged for 30 min at 277K and the supernatant was passed through a 0.45 mm filter to remove the cell debris. The supernatant was applied to a 5 mL Hi-Trap chelating HP (GE healthcare Bio-Sciences AB, Uppsala, Sweden) Ni^{+}-NTA column equilibrated in buffer 50 mM Tris-HCl pH 7.4, 300 mM NaCl, and 2 mM β-mercaptoethanol. After removal of the N-terminal hexa-histidine tag using thrombin, gel filtration was carried out on a Superdex-75s prep-grade column (GE healthcare Bio-Sciences AB) which was previously equilibrated with a buffer containing 50 mM Tris-HCl, pH 7.5, 150 mM NaCl, and 1 mM TCEP. The purified protein solution was concentrated to 10 mg ml^{-1} using an Amicon Ultra-15 (Millipore, Billerica, MA, USA). *Bc*PDF1 was prepared as previously described (Park *et al*., 2005).

Complex formation and crystallization. The purified *Bc*PDF2 in 50 mM Tris-HCl, pH 7.5, 150 mM NaCl, and 1 mM TCEP, was mixed with 2.5 mM actinonin in DMSO and incubated on ice for 1 h. Initial screening for crystallization was performed using the sitting-drop vapor diffusion method using 96-well Intelli plates (Hampton Research) and Hydra II plus one (MATRIX Technologies Corp.,) at 295K over 1200 commercially available kits. After a few days one condition gave microcrystals and the condition was optimized using the hanging drop vapor diffusion method. The well diffracting single crystals were obtained after 7 days from 1.25-1.4 M sodium citrate, pH 6.5.

Data collection and structure determination. The crystal of *Bc*PDF2-actinonin complex measuring $0.1 \times 0.15 \times 0.3$ mm^3 was used for data collection. The crystal was transferred to a solution containing 1.4 M sodium citrate pH 6.5 and 25% (v/v) glycerol before placing it in 100K nitrogen-gas stream. The crystal belongs to the space group $P6_522$ or $P6_122$ with unit cell parameters of $a = b = 69.45$ and $c = 294.41$ Å. The asymmetric unit contains two molecules of *Bc*PDF2, giving a crystal volume per protein mass (V_m) of 2.50 $Å^3$ Da^{-1} and a solvent content of 48.9% (Mathews, 1968).

The diffraction data were collected at 100K with ADSC Quantum CCD Q210 detector (ADSC, USA) at the 4A beamline of Pohang Light Source (PAL). The crystal was rotated for a total of 360° with 1° oscillation per frame and 1 s exposure per frame. The data were processed and scaled using the program HKL2000 (HKL Research Inc., Charlottesville, VA, USA) (Otwinowski & Minor, 1997). Multiwavelength anomalous diffraction (MAD) data were collected on Zn^{2+}-substituted *Bc*PDF2-actinonin complex at three wavelengths at the 6B beamline of Pohang Light Source. The positions of two Zn^{2+} ions in the asymmetric unit were located and refined using the program SOLVE and RESOLVE (Terwilliger, 2004). Crystallographic refinement was carried out with CNS (Brünger *et al*., 1998), while model building was performed using COOT (Emsley & Cowtan, 2004) and QUANTA (Accelrys Software Inc.). The figures were prepared using PyMOL (PyMOL Molecular Graphics System; Delano Scientific) and QUANTA. Final statistics for data collection and structure refinement were summarized in Table 1.

Enzymatic analysis. The enzymatic activities were measured using the coupled assay of peptide deformylase and formate dehydrogenase (FDH) activity (Lezennec and Meinnel, 1997). The formate generated by PDF from its substrate N-formyl-Met-Ala-Ser (fMAS) is oxidized by the second enzyme FDH, reducing NAD^{+} to NADH and this causes specific absorption change at 340 nm (molar extinction coefficient of 6300 M^{-1} cm^{-1}). All assays were conducted using a 96-well plate system and SPECTRA MAX 340 reader (Molecular Devices, Sunnyvale, CA, USA) at room temperature. The assay solution contained 50 mM KH_2PO_4, pH 7.5, 2 mM NAD^{+} (Sigma-Aldrich), 0.7 U/mL FDH (Sigma-Aldrich), and fMAS (Bachem) at appropriate concentrations. The reaction was initiated by adding the PDFs.

Coordinates. The atomic coordinates and structure factors have been deposited in the Protein Data Bank (The accession codes is 2OKL).

Results and Discussion

Overall structure of *Bc*PDF2. The complex structure of *Bc*PDF2-actinonin was determined using MAD phasing and refined to an *R*-value of 22.7% (R_{free} = 25.7%) at 1.7 Å resolution. The final model includes two PDF molecules, molecule A and B, four actinonin molecules, one citrate and 336 waters. All atoms for the protein as well as actinonin molecules are well defined in the electron density maps, except there is a break in the backbone at residues 169 and some of the side chains are disordered. Interestingly, one histidine residue from the tag is visible at the N-terminus of molecule A. The final statistics on the refinement are given in Table 1.

The tertiary structure of *Bc*PDF2 consists of a mixed α + β topology, with three α-helices, eight β-strands and three 3_{10} helices, as shown in Fig. 2(a). The metal ion at the active site

Table 1. Data collection and refinement statistics. Values in parentheses are for the outer most resolution shell

	*Bc*PDF2-actinonin complex	Zn^{2+}-MAD		
		Peak	Edge	Remote
Wavelength, Å	0.97123 Å. (PAL, 4A MXW)	1.2823 (PAL, 6B)	1.2828 (PAL, 6B)	1.2693 (PAL, 6B)
Resolution range, Å	50-1.65 (1.70-1.65)	50-3.0 (3.11-3.0)	50-3.0 (3.11-3.0)	50-3.0 (3.11-3.0)
Space group	$P6_522$		$P6_522$	
Unit cell parameters, Å	a = 69.45 b = 69.45 c = 294.41		a = 69.30 b = 69.30 c = 293.81	
Total/unique reflections	1212704/52252	341419/9165	335211/9194	334569/9201
Completeness (last shell), %	93.4 (78.5)	96.6 (86.9)	96.6 (85.9)	96.7 (88.9)
Mean $I/\sigma(I)$ (last shell), %	45.4 (1.54)	26.4 (5.5)	24.8 (4.5)	22.0 (3.6)
R_{merge}[a] (last shell), %	6.6 (40.2)	11.7 (27.3)	11.5 (28.4)	12.2 (33.3)

[a]$R_{merge} = \Sigma_h\Sigma_i¾I(h,i) - <I(h)>3/4/\Sigma_h\Sigma_i I(h,i)$, where $I(h,i)$ is the intensity of the i^{th} measurement of reflection h and $<I(h)>$ is the mean value of $I(h,i)$ for all i measurements.

Refinement		RMSD from ideality		Ramachandran analysis		
					A	B
Resolution range, Å	20.0-1.70	Bond lengths, Å	0.0057	Favored (%)	91.1	88.7
R_{work}/R_{free} %	22.8/25.7	Bond angles, °	1.24	Allowed (%)	8.9	10.7
No. of protein atoms	2886			Generally allowed (%)	0	0.6
No. of water molecules	336			Disallowed (%)	0	0

is located near the central α-helix. There are two independent PDF molecules, molecule A and B, in an asymmetric unit and the overall arrangement of two non-crystallographically related PDF molecules is shown in Fig. 2(b). The two molecules are almost identical with an r.m.s. deviation of 0.34 Å for 183 C_α atoms. *Bc*PDF2 clearly belongs to the type II with the C-terminal end forming a β-structure instead of an α-helix as seen in type I. The r.m.s. deviations to other type II PDFs are: 0.77 Å for 182 C_α atoms of *B. Strearothermophilus* PDF (Guilloteau *et al*., 2002) (PDB code: 1LQY); 0.89 Å for 176 C_α atoms of *S. pneumoniae* PDF (Kreusch *et al*., 2003) (PDB code: 1LM6) and 0.96 Å for 179 C_α atoms of *S. aureus* PDF (Guilloteau *et al*., 2002) (PDB code: 1LQW) with the sequence identities of 70, 52 and 58%, respectively. The major difference between *B. Strearothermophilus* PDF and *B. cereus* PDF is at the C-terminal end; five or so residues at the C-terminal have moved away from the active site of the molecule in the case of *Bc*PDF2 and this is most probably due to actinonin binding at the interface.

Quaternary structure of *Bc*PDF2. The two molecules in an asymmetric unit form a dimer related by a non-crystallographic two fold axis. The interaction mainly involves the C-terminal 10 or so residues (173-184) of the first molecule packed against the residues of 45-56 and the 'CD loop' of the second molecule. The dimerization surface involves both strong hydrophobic interactions as well as a network of hydrogen bonds. One notable thing from the early stage of the refinement was that both 2Fo-Fc and Fo-Fc maps clearly revealed two actinonin molecules at the interface region in addition to the actinonin molecules bound at the active site of the enzyme. Figure 2(b) shows the 2Fo-Fc map at the interface. In addition, there are about 40 tightly bound water molecules at the interface. Therefore, the interactions seen at the interface are quite extensive involving protein-protein, protein-inhibitor, inhibitor-inhibitor interactions as well as water mediated interactions. A total of about 1450 $Å^2$ of accessible surface gets buried upon dimerization and this corresponds to about 15% of the surface area of a PDF monomer. If one excludes the two actinonin molecules at the interface, the corresponding value becomes about 950 $Å^2$ which is still significant indicating extensive interaction between the molecules. However, *Bc*PDF2 behaves as a monomer in gel filtration experiments with an apparent molecular mass of 20 ± 3 kDa as well as in the non-denaturing PAGE (data not shown). Therefore, it is tempting to suggest that *Bc*PDF2 exists as a monomer in the solution, but the dimeric structure seen here may well be an outcome of crystal packing.

PDFs from *Leptospira interrogans* (Zhou *et al*., 2004) (PDB code: 1Y6H) and mitochondria (Type 1A) from *Arabidopsis thaliana* (Fieulaine *et al*., 2005) (PDB code: 1ZY1) are reported to exist as a dimer both in the crystal form and in solution. The orientation of the two PDF molecules in *Li*PDF and *At*PDF is quite similar to each other. In both cases the

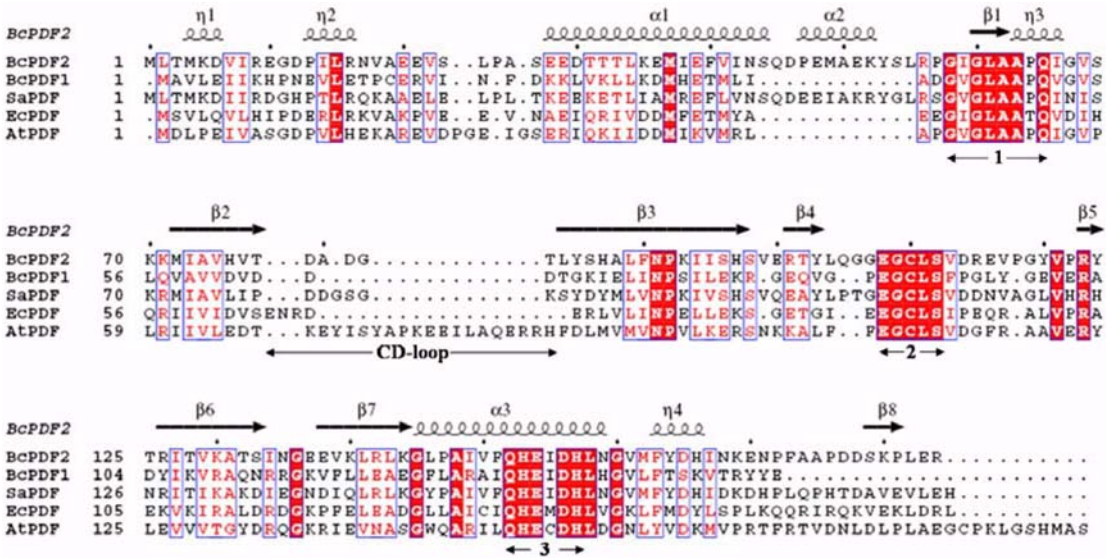

Fig. 1. Sequence Alignment. Peptide deformylases from *Bacillus cereus, Bc*PDF2 *and Bc*PDF1*, S. aureus* PDF, *E. coli* PDF *and Arabidopsis thaliana* PDF1A. Sequence alignment is based on the structural elements and the secondary structure of *Bc*PDF2 is shown on the top. The three conserved stretches of PDFs as well as the CD loop are indicated with at the bottom. This figure was created with ESPript [30].

interface involves both strong hydrophobic interactions and a network of hydrogen bonds. The clusters of hydrophobic residues, phenylalanines and methionines, at the center of the interface seem to play a critical role in dimerization, and there are only a few water molecules at the interface in both, contrasting from what is observed in *Bc*PDF2 dimer interface. The subunit contact areas in these two structures are reported as 800 $Å^2$ and 1060 $Å^2$ per monomers, respectively, and they correspond to about 10% of the solvent accessible surface area of the corresponding monomer. Also the arrangement of the dimer in these two is significantly different from that of *Bc*PDF2 dimer, although it also involved C-terminal end, residues beyond the helix α3, of the molecule (see Fig. 1).

Comparison of *Bc*PDF1 and *Bc*PDF2. The enzymatic activity of *Bc*PDF1 and *Bc*PDF2 biochemical data shows that both enzymes catalyze peptide deformylation of fMAS, the substrate. However, PDF2 is far more active than PDF1 as shown in Fig. 3. The kinetic parameters for *Bc*PDF2 are k_{cat} of 0.161 s^{-1} and K_M of 2.73 mM. The K_M values and the apparent turnover numbers are 2.3 mM and 3.0 mM and 0.17 s^{-1} and 0.07 s^{-1}, respectively (Haas *et al*., 2001). Also the two PDFs showed similar IC_{50} values for actinonin - the values being 95 nM and 130 nM, respectively. To investigate the metal dependency on the enzymatic activity, we prepared Zn^{2+}, Co^{2+} and Ni^{2+} substituted enzymes by culturing *E. coli* cells in LB media supplemented with 100 μM $CoCl_2$, $ZnCl_2$, and $NiSO_4$. The result shows that both *Bc*PDF1 and *Bc*PDF2 show the same trend, $Ni^{2+} > Co^{2+} > Zn^{2+}$. The metal dependency of PDFs varies from one to the other, e.g. *E. coli* PDF is active with ferrous ion and not Zn^{2+} (Rajagopalan *et al*., 1997; Ragusa *et al*., 1998), *L. interrogans* PDF shows almost the opposite effect of $Zn^{2+} > Fe^{2+} > Co^{2+} \sim Ni^{2+}$ (Li *et al*., 2002) while PDF from *H. pylori* showed a similar trend ($Co^{2+} > Zn^{2+}$) (Han *et al*., 2004).

The overall structure of *Bc*PDF2 is similar to *Bc*PDF1 reported earlier (Moon *et al*., 2005) except for the C-terminal and a few places with insertions despite the low sequence identity as seen in Fig. 4(a). The C-terminal of PDF1 forms a β-structure as in PDF2, but it is much shorter and heads the opposite direction. The major insertion is a 12 residue-long stretch between the α1 helix and β1 strand. PDF2 has 3 extra residue insertions for the 'CD loop' and another insertion after the β4 strand. The r.m.s. deviation between molecule A of PDF1 and PDF2 is 1.5 Å for 144 C_α atoms. In fact, *Bc*PDF1 does not belong to neither type I nor type II.

The active site of *Bc*PDF2 has clearly bound actinonin as shown in Fig. 2(b). In both molecules A and B the metal ion (Zn^{2+}) is pentahedrally coordinated by Cys110, His153, His157 and the both oxygen atoms of hydroxamate moiety from actinonin. This is similar to what has been observed in other actinonin bound structures - both type I and type II. The binding pockets for the tightly bound actinonin (and substrate) are made of residues from the helices α3, α4 and the strands β1, β3 and β4 and most of these residues are conserved (Fig. 1). Actinonin makes hydrogen bonds with Ile59, Gln65, Gly107, Gly109, Leu111, Glu154 and His157, which are all conserved in PDFs.

When the active site of *Bc*PDF2 is compared to that of *Bc*PDF1, the metal-binding site is almost identical as seen in Fig. 4(b). All the residues coordinating the metal and the immediate residues are highly conserved as seen in Fig. 1. In fact, the three conserved stretches, i.e. GxGxAAxQ, EGCLS and QHExDHxxG, define the catalytic domain of deformylase.

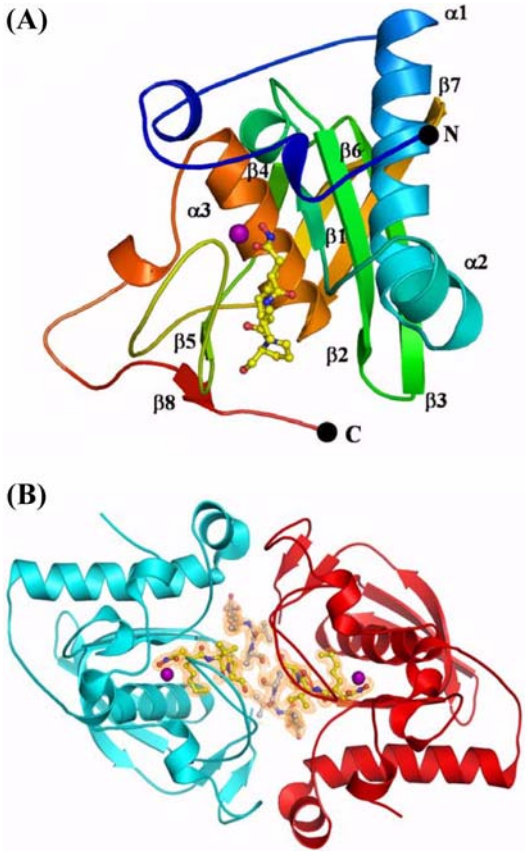

Fig. 2. Structure of *Bc*PDF2. (A) Ribbon representation of the *Bc*PDF2 is color coded from blue (N-terminus) to red (C-terminus). The Zn^{2+} ion is shown as a sphere in magenta and actinonin is displayed as ball-and-stick model with carbon atoms shown in yellow, oxygen in red and nitrogen in blue. (B) Overall arrangement of PDF molecules in an asymmetric unit. The two molecules are related by non-crystallographic 2-fold axis. The two additional actinonin molecules are found at the interface region and they are shown over the 2Fo-Fc electron density map contoured at 1σ level.

These are indicated at the bottom of the sequence alignment in Fig. 1. Unlike in *B. cereus* and *B. subtilis*, only one of the PDFs from *S. aureus* and *S. pneumoniae* are active due to the fact that the required residues for the metal biding and catalysis in the three stretches are replaced (Margolis, 2000 & 2001). However, in the case of *Bc*PDF1 and *Bc*PDF2, although the overall structure and the key residues at the active site are identical in the two, there are differences in the binding pockets. One of the major differences is in the S1' pocket - the residues lining the pocket are Ile59, Leu146, Ile149 and Val150 in *Bc*PDF2 while they are Val, Phe, Arg and Ala in *Bc*PDF1. These differences between the two isoforms are found in other *Bacillus* PDFs. Interestingly, the corresponding residues are Val48, Trp146, Arg149 and Ile150 in *A. thaliana* and human PDF. The side chain of Arg56 at the end of the 12-residue long insertion in PDF2 is located at the tip of P2', and therefore might influence the substrate binding.

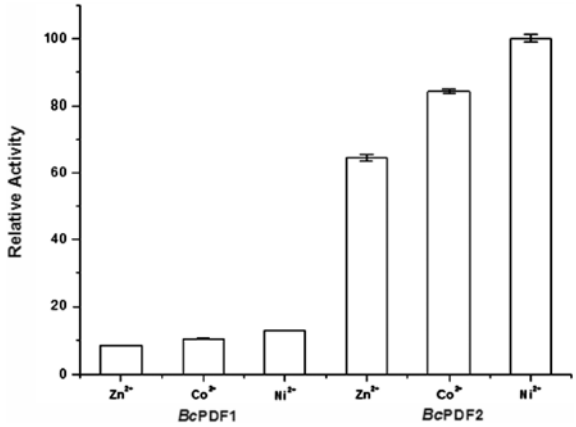

Fig. 3. Enzyme activity of PDFs. In order to see the effect of the different metal ions on the enzymatic activities of *Bc*PDF1 and *Bc*PDF2, Zn^{2+}, Co^{2+} and Ni^{2+} substituted enzymes were prepared by culturing *E. coli* cells in LB media supplemented with 100 μM $CoCl_2$ and $NiSO_4$.

In addition, the 3 residue insertion after β4 is near the S1' and S3' pocket. So these structural differences might influence the enzymatic properties of the two.

Conformation of Actinonin. There are four crystallographically independent actinonin molecules in the structure: two at the active site and two at the dimer interface. They are in close proximity with each other as shown in Fig. 2(B) and Fig. 4(D). The active site actinonin molecule makes various hydrogen bonds to protein in addition to coordinating the metal ion as mentioned above. However, the actinonin molecule at the interface does not make much specific interactions. It makes a direct hydrogen bond to the second interface actinonin molecule and an indirect hydrogen bond to the active site actinonin via a water molecule. The hydroxamate moiety makes only one H-bond to the guanidinium group of Arg184. Otherwise the side chains of Leu104, Gln105 and Gly106 of molecule A and Pro57, Ile59, Thr78 and Leu146 of molecule B are close by making hydrophobic interaction. So, the conformation of the interface actinonin adopts a quite different conformation from that of the active site actinonin as shown in Fig. 5. Considering the fact that the hydroxamate moiety is used as the basis for many inhibitors targeting PDF (Apfel *et al*., 2000) as well as other zinc metalloproteases, matrix metalloproteinases, leukotrien A hydrolases, ureases, lipoxigenase to name a few (Muri *et al*., 2002; Lou and Yang, 2003), it is striking to see how flexible this moiety can be when it is not coordinating a metal ion.

Conclusions

Here we reported the crystal structure of *Bc*PDF2 complexed with actinonin, a natural potent inhibitor. The enzymatic activity result shows that *Bc*PDF2 is far more active than

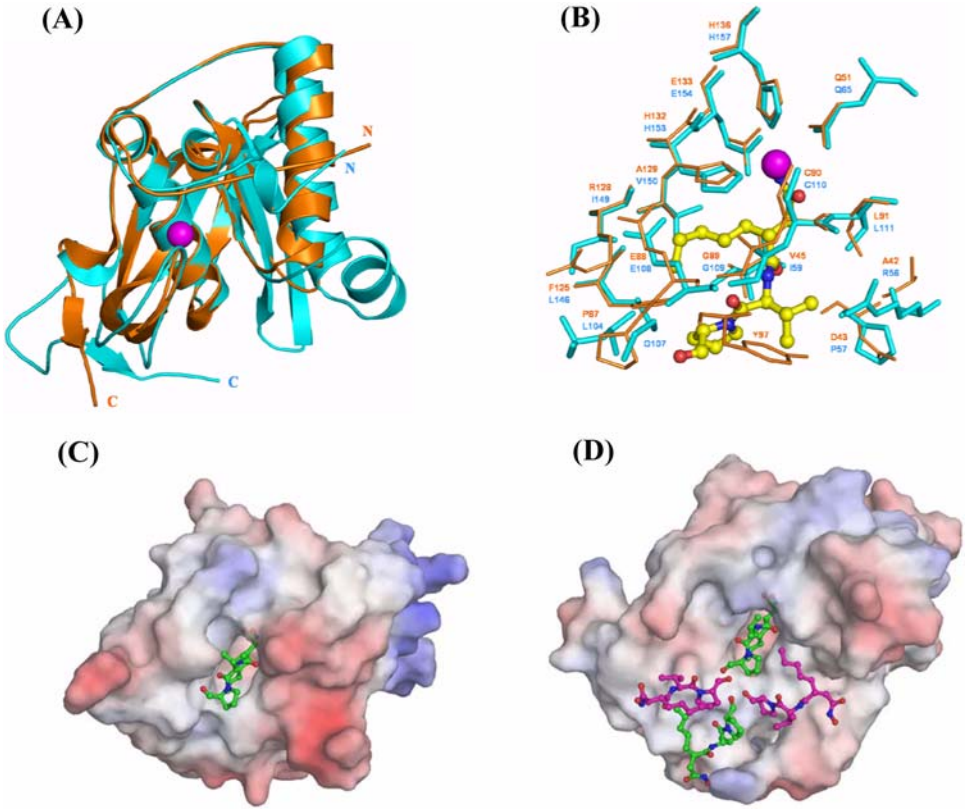

Fig. 4. Comparison of *Bc*PDF1 and *Bc*PDF2. (A) Overall structure and (B) the active site of *Bc*PDF1, shown in orange, and *Bc*PDF2, shown in cyan. The active site of *Bc*PDF1(shown in thin line) is superimposed onto the molecule of A of *Bc*PDF2 (shown in thick line). Superposition was done using QUANTA based on the sequence alignment. Molecular surface of *Bc*PDF1 (C) and *Bc*PDF2(D). The two actinonin molecules at the interface are shown in purple.

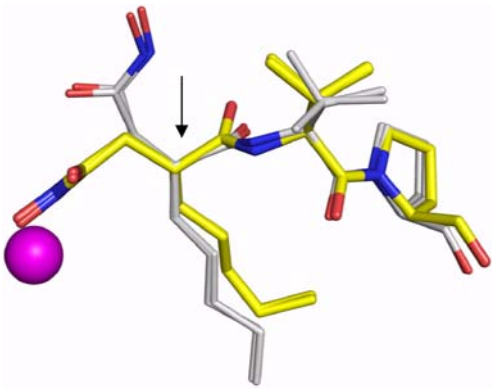

Fig. 5. Conformation of the Actinonin. Two actinonin molecules bound at the active site are shown in yellow tone while the two actinonin molecules located at the interface are shown in grey tone. The metal ion is shown as a solid sphere in magenta and oxygen atoms are in red while the nitrogen atoms are in blue. The superimposition results from the overlay made with the three adjacent carbon atoms from the carbon atom indicated by an arrow.

*Bc*PDF1, and there appears to be a clear metal preference in the order $Ni^{2+} > Co^{2+} > Zn^{2+}$. The overall structure of the two isozymes is similar despite low sequence identity between the two, but *Bc*PDF2 belongs to type II while *Bc*PDF1 belongs to neither type I nor type II. The residues chelating the metal ion are conserved, however, the lining of the substrate binding pockets differ slightly between the two and these differences probably reflects the difference in the activity shown. In addition, *Bc*PDF2 is found as a dimer with two additional actinonin molecules bound at the interface, despite the fact that it behaves as a monomer in solution.

Acknowledgments This work was financially supported by the Functional Proteomics Center, the 21C Frontier Research & Development Program of the Korea Ministry of Science and Technology and the Chemoinformatics grant from Korea Institute of Science and Technology. We thank the staffs for assistance during data collection at BL-6B and BL-4A, Pohang Light Source, Korea.

References

Apfel, C., Banner, D. W., Bur, D., Dietz, M., Hiraa, T., Hubschwerlen, C. Locher H., Page, M. G., Pirson, W., Rosse, G. and Specklin, J. L. (2000) Hydroxamic acid derivatives as potentent peptide deformylase inhibitors and antibacterial agents.

J. Med. Chem. **43**, 2324-2331.

Ball, L. A. and Kaesberg, P. (1973) Cleavage of the N-terminal formylmethionine residue from a bacteriophage coat protein in vitro. *J. Mol. Biol.* **79**, 531-537.

Baldwin, E. T., Harris, M. S., Yem, A. W., Wolfe, C. L., Vosters, A. F., Curry, K. A., Murray, R. W., Bock, J. H., Marshall, V. P., Cialdella, J. I., Merchant, M. H., Choi, G. and Deibel Jr, M. R. (2002) Crystal structure of type II peptide deformylase from *Staphylococcus aureus*. *J. Biol. Chem.* **277**, 31163-31171.

Becker, A., Schlichting, I., Kabsch, W., Groche, D., Schultz, S. and Wagner, A. F. V. (1998) Iron center, substrate recognition and mechanism of peptide deformylase. *Nat. Struct. Biol.* **5**, 1053-1058.

Brünger, A. T., Adams, P. D., Clore, G. M., DeLano, W. L., Gros, P., Grosse-Kunstleve, R. W., Jiang, J. S., Kuszewski, J., Nilges, M., Pannu, N. S., Read, R. J., Rice, L. M., Simonson, T. and Warren, G. L. (1998) Crystallography & NMR system: a new software suite for macromolecular structure determination. *Acta Crystallogr. D Biol. Crystallogr.* **54**, 905-921.

Chen, D. Z., Patel, D. V., Hackbarth, C. J., Wang, W., Dreyer, G., Young, D. C., Margolis, P. S., Wu, C., Ni, Z. J., Trias, J., White, R. J. and Yuan, Z. (2000) Actinonin, a naturally occurring antibacterial agent, is a potent deformylase inhibitor. *Biochemistry* **39**, 1256-1262.

Ednie, L. M., Pankuch, G. and Appelbaum, P. C. (2004) Antipneumococcal activity of LBM415, a new peptide diformylase inhibitor, compared with those of other agents. *Antimicrob. Agents Chemother.* **48**, 4027-4032.

Emsley, P. and Cowtan, K. (2004) Coot: model-building tools for molecular graphics. *Acta Crystallogr. D Biol. Crystallogr.* **60**, 2126-2132.

Fieulaine, S., Juillan-Binard, C., Serero, A., Dardel, F., Giglione, C., Meinnel, T. and Ferrer, J. L. (2005) The crystal structure of mitochondrial (Type 1A) peptide deformylase provides clear guidelines for the design of inhibitors specific for the bacterial forms. *J. Biol. Chem.* **280**, 42315-42324.

Giglione, C., Serero, A., Pierre, M., Boisson, B. and Meinnel, T. (2000) Identification of eukaryotic peptide deformylases reveals universality of N-terminal protein processing mechanism. *EMBO J.* **19**, 5916-5929.

Gouet, P., Courcelle, E., Stuart, D. I. and Metoz, F. (1999) ESPript: analysis of multiple sequence alignments in PostScript. *Bioinformatics* **15**, 305-308.

Guilloteau, J. P., Mathieu, M., Giglione, C., Blanc, V., Dupuy, A., Chevrier, M., Gil, P., Famechon, A., Meinnel, T. and Mikol, V. (2002) The crystal structures of four peptide deformylases bound to the antibiotic actinonin reveal two distinct types: a platform for the structure-based design of antibacterial agents. *J. Mol. Biol.* **320**, 951-962.

Haas, M., Beyer, D., Gahlmann, R. and Freiberg, C. (2001) YrkB is the main peptide deformylase in *Bacillus subtilis*, a eubacterium containing two functional peptide deformylases. *Microbiology* **147**, 1783-1791.

Han, C., Wang, Q., Dong, L., Sun, H., Peng, S., Chen, J., Yang, Y., Yue, J., Shen, X. and Jiang, H. (2004) Molecular cloning and characterization of a new peptide deformylase from human pathogenic bacterium *Helicobacter pylori*. *Biochem. Biophy. Res. Commun.* **319**, 1292-1298.

Jain, R., Chen, D., White, R. J., Patel, D. V. and Yuan, Z. (2005) Bacterial peptide deformylase inhibitors: a new class of antibacterial agents. *Curr. Med. Chem.* **12**, 1607-1621.

Kreusch, A., Spraggon, G., Lee, C. C., Klock, H., McMullan, D., Ng, K., Shin, T., Vincent, J., Warner, I., Ericson, C. and Lesley, S. A. (2003) Structure analysis of peptide deformylases from *Streptococcus pneumoniae*, *Staphylococcus aureus*, *Thermotoga maritima* and *Pseudomonas aeruginosa*: snapshots of the oxygen sensitivity of peptide deformylase. *J. Mol. Biol.* **330**, 309-321.

Lazennec, C and Meinnel, T. (1997) Formate dehydrogenase-coupled spectrophotometric assay of peptide deformylase. *Anal. Biochem.* **244**, 180-182.

Leeds, J. A. and Dean, C. R. (2006) Peptide deformylase as an antibacterial target: a critical assessment. *Curr. Opin. Pharmacol. Rev.* **6**, 445-452.

Li, Y., Chen, Z. and Gong, W. (2002) Enzymatic properties of a new peptide deformylase from pathogenic bacterium *Leptospira interrogans*. *Biochem. Biophy. Res. Commun.* **295**, 884-889.

Lofland, D., Difuntorum, S., Waller, A., Clements, J. M., Weaver, M. K., Karlowsky, J. A. and Johnson, K. (2004) Related Articles, *In vitro* antibacterial activity of the peptide deformylase inhibitor BB-83698. *J. Antimicrob. Chemother.* **53**, 664-668.

Lou, B. and Yang, K. (2003) Molecular diversity of hydroxamic acids: part II. Potential therapeutic applications. *Mini Rev. Med. Chem.* **3**, 609-620.

Margolis, P. S., Hackbarth, C. J., Young, D. C., Wang, W., Chen, D., Yuan, Z., White, R. and Trias, J. (2000) Peptide deformylase in *Staphylococcus aureus*: resistant to inhibition is mediated by mutations in the formyl transferase gene. *Antimicrob. Agents Chemother.* **44**, 1825-1831.

Margolis, P. S., Hackbarth, C. J., Lopez, S., Maniar, M., Wang, W., Yuan, Z., White, R. and Trias, J. (2001) Resistance of *Streptococcus pneumoniae* to deformylase inhibitors is due to mutation in *defB*. *Antimicrob. Agents Chemother.* **45**, 2432-2435.

Matthews, B. W. (1968) Solvent content of protein crystals. *J. Mol. Biol.* **33**, 491-497.

Moon, J. H., Park, J. K. and Kim, E. E. (2005) Structure analysis of peptide deformylase from *Bacillus cereus*. *Proteins* **61**, 217-220.

Muri, E. M., Nieto, M. J. Sinderlar, R. D. and Williamson, J. S. (2002) Hydroxamic acids as pharmacological agents. *Curr. Med. Chem.* **9**, 1631-1653.

Otwinowski, Z. and Minor, W. (1997) Processing of X-ray diffraction data collected on oscillation mode. *Methods Enzymol.* **276**, 307-326.

Park, J. K., Moon, J. H., Kim, J. H. and Kim, E. E. (2005) Crystallization and preliminary X-ray crystallographic analysis of peptide deformylase (PDF) from *Bacillus cereus* in ligand free and actinonin-bound forms. *Acta Crystallogr. Sect F.* **61**, 150-152.

Ragusa, S., Blaquet, S. and Meinnel, T. (1998) Control of peptide deformylase activity by metal cations. *J. Mol. Biol.* **280**, 515-523.

Rajagopalan, P. T. R., Yu, X. C. and Pei, D. (1997) Peptide deformylase: a new type of mononuclear iron protein. *J. Am. Chem. Soc.* **119**, 12418-12419.

Srivaths, P. R., Rozans, M. K., Kelly Jr, E. and Venkateswaran, L. (2004) *Bacillus cereus* central line infection in an immuno-competent child with hemophilia. *J. Pediatr. Hematol. Oncol.* **26**, 194-196.

Terwilliger, T. (2004) SOLVE and RESOLVE: automated structure solution, density modification and model building. J. *Synchrotron Radiat.* **11**, 49-52.

Yuan, Z. and White, R. J. (2006) The evolution of peptide deformylase as a target: contribution of biochemistry, genetics

and genomics. *Biochem. Pharmacol. Rev.* **71**, 1042-1047.
Zhang, X., Zhang, S., Hao, F., Lai, X., Yu, H., Huang, Y. and Wang, H. (2005) Expression, purification and properties of Shikimate dehydrogenase from *Mycobacterium Tuberculosis*. *J. Biochem. Mol. Biol.* **38**, 624-631.
Zhou, Z., Song, X., Li, Y. and Gong, W. (2004) Unique structural characteristics of peptide deformylase from pathogenic bacterium *Leptospira interrogans*. *J. Mol. Biol.* **339**, 207-215.